ACADEMIC PRESS

Available online at www.sciencedirect.com

SCIENCE DIRECT®

Journal of Sound and Vibration 263 (2003) 979–1003

JOURNAL OF SOUND AND VIBRATION

www.elsevier.com/locate/jsvi

Free vibration analysis of corner-supported rectangular plates with symmetrically distributed edge beams

D.J. Gorman*

Department of Mechanical Engineering, University of Ottawa, Ottawa, Canada K1N 6N5

Accepted 4 February 2003

Abstract

Analytical type solutions are obtained for the free vibration frequencies and mode shapes of thin corner-supported rectangular plates with symmetrically distributed reinforcing beams, or strips, attached to the plate edges. The method of superposition is employed. Equations governing reactions at plate–beam interfaces are developed in dimensionless form. The approach is comprehensive in that both lateral and rotational stiffness, and inertia, of the beam are incorporated into the analysis. For illustrative purposes computed eigenvalues and mode shapes are presented for two plate–beam systems of realistic geometries. It is shown that the method is easily extended to cover the case where the edge beams do not have a symmetrical distribution. This appears to be the first comprehensive analytical study of this problem of industrial interest.

1. Introduction

In this paper, exploiting the superposition method, analytical type solutions are obtained for the free vibration frequencies and mode shapes of corner-supported rectangular plates with symmetrically distributed reinforcing beams running along the plate edges. It will be seen that the analysis described is easily extended to handle the slightly more general case where the edge beams are not symmetrically distributed. Beam reinforcement is treated in the most general case, i.e., the analysis permits taking into account both bending and rotational stiffness of the beams as well as their lateral and rotational inertia. Verification of the analytical technique is achieved by demonstrating that plate eigenvalues approach correct known limits as beam properties approach the limits of zero, or infinity.

*Tel.: +1-613-562-5800/6279.
E-mail address: dgorman@eng.uottawa.ca (D.J. Gorman).

0022-460X/03/$ - see front matter
doi:10.1016/S0022-460X(03)00269-4

Eigenvalues for a typical corner-supported plate with edge beams of realistic sizes are tabulated so that other researchers and designers will have accurate results against which their findings may be compared.

A search of the literature uncovers very few publications immediately related to the problem of establishing free vibration frequencies and mode shapes of rectangular plates with edge-beam reinforcement and with, or without, corner supports. The first publication appears to be one authored by Cox and Benfield [1]. In this 1959 paper they investigated fundamental frequencies only, for square isotropic plates with pinpoint support at the corners and flexible beams running along the plate edges. The beams were considered to be pinned to the plate so that only forces related to beam flexure were transmitted to the plate. Beam rotational stiffness was not taken into consideration and effects of beam lateral and rotational inertia were neglected. A theoretical study of the problem was carried out by means of a finite difference approach.

Elishakoff and Sternberg investigated effects of attached edge beams on rectangular plates in a 1980 publication [2]. Their plates were reinforced by beams running along two opposite edges, the other two edges being given simple support. In restricting their study to plates with two opposite simply supported edges they were able to obtain an exact solution. Their problem differs significantly, of course, from the problem under study here. Nevertheless, they have provided a fairly extensive review of the literature pertinent to their problem, up to that time. Elishakoff et al., also describe some work of Sternberg in which limited results are provided for free vibration of plates with 'All-Round' I-Beam edge stiffeners [3]. Apparently beam inertia effects were neglected.

There are numerous publications in the literature related to plates reinforced with beams running along the plate lateral surface and parallel to a pair of edges. It is found, however, that such publications throw little light on the problem immediately at hand.

2. Mathematical procedure

Because of symmetry in distribution of the edge beams, i.e., opposite pairs of edges will be reinforced with identical beams, It is recognized that all free vibration modes will either be symmetric or antisymmetric with respect to the plate central axes, or symmetric about one axis and antisymmetric about the other. These three families of modes will be analyzed separately and this can be accomplished by focusing attention on one quarter of the plate only.

2.1. Formulation of the plate boundary conditions

A typical rectangular quarter-plate of interest, with reinforcing edge beams, is depicted schematically in Fig. 1.

Focusing attention on the edge, $y = b$ ($\eta = 1$), Timoshenko and Woinowsky-Kreiger have shown that, following standard nomenclature, and enforcing continuity of transverse shear forces at the beam–plate interface, one may write (neglecting inertia forces) [4]

$$E_B I \frac{\partial^4 w(x,y)}{\partial x^4}\bigg|_{y=b} = D\frac{\partial}{\partial y}\left[\frac{\partial^2 w(x,y)}{\partial y^2} + (2-\nu)\frac{\partial^2 w(x,y)}{\partial x^2}\right]\bigg|_{y=b}, \tag{1}$$

where all symbols are as defined in Appendix A.

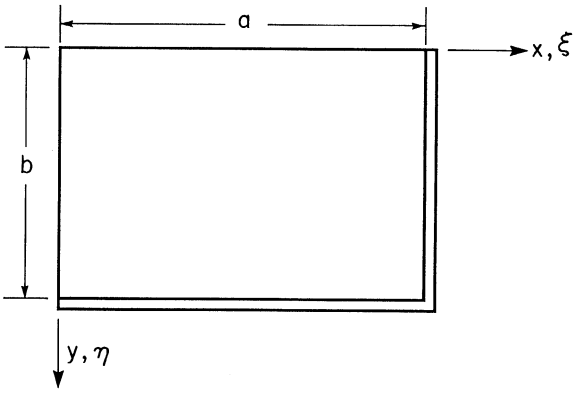

Fig. 1. Schematic view of quarter-plate with reinforcing edge-beams.

Furthermore, enforcement of continuity of bending moment across the same interface, permits one to write [4]

$$GJ_0\frac{\partial}{\partial x}\frac{\partial^2 w(x,y)}{\partial x\partial y}\bigg|_{y=b} = D\left[\frac{\partial^2 w(x,y)}{\partial y^2} + v\frac{\partial^2 w(x,y)}{\partial x^2}\right]\bigg|_{y=b}. \tag{2}$$

It will be appreciated that the quantities on the right-hand side of Eqs. (1) and (2), represent the negative of the plate vertical edge reaction and bending moment, respectively.

It is highly advantageous to express these equations in dimensionless form. Following the non-dimensionalizing procedure as utilized in an earlier publication by the author one may express Eqs. (1) and (2), respectively, as [5]

$$\frac{Vb^3}{aD}\bigg|_{\eta=1} = -Q_{11}\frac{\partial^4 W(\xi,\eta)}{\partial\xi^4}\bigg|_{\eta=1} \tag{3}$$

and

$$\frac{Mb^2}{aD}\bigg|_{\eta=1} = -G_{11}\frac{\partial^2}{\partial\xi^2}\frac{\partial W(\xi,\eta)}{\partial\eta}\bigg|_{\eta=1}, \tag{4}$$

where

$$Q_{11} = \frac{E_b I b^3}{a^4 D} \quad \text{and} \quad G_{11} = \frac{GJ_0 b}{a^2 D}.$$

The subscripted coefficients Q and G are utilized in connection with expressing lateral and rotational equilibrium, respectively.

Here, the first subscript refers to the plate edge, with subscripts 1 and 2 referring to edges, $\eta = 1$ and $\xi = 1$, respectively. In what is to follow the second subscript will be set equal to 1 when referring to beam lateral or rotational stiffness, as in Eqs. (3) and (4). The second subscript will be set equal to 2 when referring to beam lateral or rotational inertia.

It is appropriate to next formulate the counterparts of Eqs. (3) and (4) as they apply to the edge, $\xi = 1$. It is readily shown that these equations may be written as

$$\left.\frac{Va^2}{D}\right|_{\xi=1} = -Q_{21}\left.\frac{\partial^4 W(\xi,\eta)}{\partial\eta^4}\right|_{\xi=1} \tag{5}$$

and

$$\left.\frac{Ma}{D}\right|_{\xi=1} = -G_{21}\left.\frac{\partial^2}{\partial\eta^2}\frac{\partial W(\xi,\eta)}{\partial\xi}\right|_{\xi=1}, \tag{6}$$

where

$$Q_{21} = \frac{E_B I a^3}{b^4 D} \quad \text{and} \quad G_{21} = \frac{GJ_0 a}{b^2 D}.$$

The components of vertical edge reaction and bending moment required to balance the lateral and rotational inertia of the edge beams are examined next.

Again, attention is first focused on the edge, $\eta = 1$. It will be apparent that satisfaction of lateral equilibrium permits one to write in dimensional form

$$V|_{y=b} = -m\left.\frac{\partial^2 w(x,y)}{\partial t^2}\right|_{y=b}, \tag{7}$$

where m is the beam mass per unit length. Because lateral motion of the plate is harmonic of circular frequency ω we may re-write Eq. (7) as

$$V|_{y=b} = m\omega^2 w(x,y)|_{y=b}. \tag{8}$$

In order to write Eq. (8) in dimensionless form it is convenient to represent the mass per unit length of the beam as the product $A_B\rho_B$, where A_B is the beam cross-sectional area and ρ_B is its density. Also recall the definition of λ^2, the dimensionless frequency of vibration.

It is then readily shown that Eq. (8) may be written in dimensionless form as

$$\left.\frac{Vb^3}{aD}\right|_{\eta=1} = Q_{12} W(\xi,\eta)|_{\eta=1} \tag{9}$$

with the corresponding equation applicable along the edge, $\xi = 1$, becoming

$$\left.\frac{Va^2}{D}\right|_{\xi=1} = Q_{22} W(\xi,\eta)|_{\xi=1}, \tag{10}$$

where

$$Q_{12} = \frac{A_B\rho_B b^3\lambda^4}{\rho_P a^4 h} \quad \text{and} \quad Q_{22} = \frac{A_B\rho_B\lambda^4}{a\rho_P h}.$$

Finally, turning to the component of edge moment required to balance the beam rotary inertia and again beginning by focusing attention on the edge, $\eta = 1$, it will be apparent that satisfaction of rotational equilibrium permits one to write in dimensional form

$$M|_{y=b} = J\rho_B\left.\frac{\partial^2}{\partial t^2}\frac{\partial w(x,y)}{\partial y}\right|_{y=b} \tag{11}$$

or

$$M|_{y=b} = -J\rho_B\omega^2 \left.\frac{\partial w(x,y)}{\partial y}\right|_{y=b}. \tag{12}$$

Non-dimensionalizing in a manner similar to that used in handling lateral inertia we find that Eq. (12) becomes

$$\left.\frac{Mb^2}{aD}\right|_{\eta=1} = -G_{12} \left.\frac{\partial W(\xi,\eta)}{\partial \eta}\right|_{\eta=1} \tag{13}$$

with the corresponding equation applicable along the edge, $\xi = 1$, becoming

$$\left.\frac{Ma}{D}\right|_{\xi=1} = -G_{22} \left.\frac{\partial W(\xi,\eta)}{\partial \xi}\right|_{\xi=1}, \tag{14}$$

where

$$G_{12} = \frac{J\rho_B b\lambda^4}{\rho_P a^4 h} \quad \text{and} \quad G_{22} = \frac{J\rho_B \lambda^4}{\rho_P a^3 h}.$$

This completes the formulation of all boundary conditions required for the plate vibration problem under study.

It is appropriate here to point out that in the above formulation of boundary conditions, and as formulated by Timoshenko and Woinowsky-Kreiger for static problems, it is assumed that the central axis of the beam coinsides with the plate edge. This is equivalent to assuming that the beam central axis lies along the mid-plane of the plate and that plate lateral dimensions are large in comparison to the edge-beam widths.

2.2. Symmetric mode free vibration analysis

In employing the superposition method it is necessary to choose an appropriate set of rectangular plate forced vibration solutions (building blocks) for which Levy-type solutions exist. These solutions are then superimposed and constants contained therein are constrained in order to satisfy the prescribed boundary conditions.

A solution for fully symmetric modes of the plate of current interest is obtained by superimposing the set of six building blocks depicted schematically in Fig. 2. Two small open circles adjacent to an edge indicate that it is given slip-shear support. This implies that vertical edge reaction, and slope taken normal to the boundary, are everywhere zero.

The edge, $\eta = 1$, of the first building block is free of vertical edge reaction. It is subjected to a distributed forced harmonic edge rotation of circular frequency ω.

It is known that a solution for the amplitude of response of this building block can be expressed as

$$W(\xi,\eta) = \sum_{m=1,2}^{\infty} Y_m(\eta)\cos(m-1)\pi\xi. \tag{15}$$

Upon substituting this solution into the plate governing differential equation it is found that the space variables are separable and the functions $Y_m(\eta)$ must satisfy the ordinary

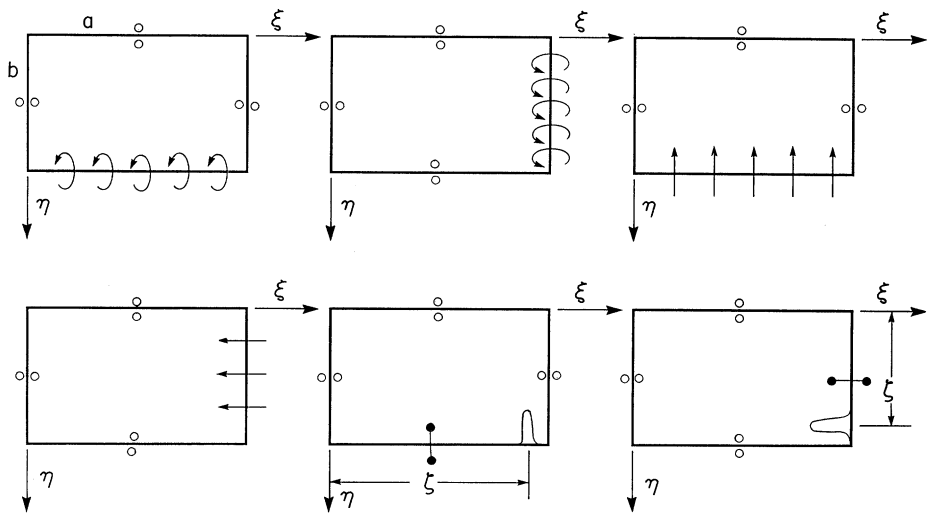

Fig. 2. Schematic representation of building blocks employed in fully symmetric mode analysis.

differential equation

$$\frac{\mathrm{d}^4 Y_m(\eta)}{\mathrm{d}\eta^4} - 2\phi^2((m-1)\pi)^2\frac{\mathrm{d}^2 Y_m(\eta)}{\mathrm{d}\eta^2} + \phi^4[((m-1)\pi)^4 - \lambda^4]Y_m(\eta) = 0. \tag{16}$$

It follows that solutions for the functions $Y_m(\eta)$ are expressed as

For $\lambda^2 > ((m-1)\pi)^2$:

$$Y_m(\eta) = A_m \sinh \beta_m\eta + B_m \cosh \beta_m\eta + C_m \sin \gamma_m(\eta) + D_m \cos \gamma_m\eta. \tag{17}$$

For $\lambda^2 < ((m-1)\pi)^2$:

$$Y_m(\eta) = A_m \sinh \beta_m\eta + B_m \cosh \beta_m\eta + C_m \sinh \gamma_m\eta + D_m \cosh \gamma_m\eta, \tag{18}$$

where

$$\beta_m^2 = \varphi^2\{\lambda^2 + ((m-1)\pi)^2\} \quad \text{and} \quad \gamma_m^2 = \phi^2\{\lambda^2 - ((m-1)\pi)^2\}$$

or

$$\phi^2\{((m-1)\pi)^2 - \lambda^2\}, \text{ whichever is positive.}$$

A_m and B_m, etc. are constants to be evaluated.

In view of the boundary conditions imposed along the edge, $\eta = 0$, of the present building block, it will be obvious that all sine and hyperbolic sine terms must vanish. Two boundary conditions are available for evaluation of the remaining two constants.

The condition of zero vertical edge reaction along the driven edge is expressed in dimensionless form as [5]

$$\frac{\partial^3 W(\xi,\eta)}{\partial\eta^3} + \nu^*\phi^2\left.\frac{\partial^3 W(\xi,\eta)}{\partial\eta\partial\xi^2}\right|_{\eta=1} = 0. \tag{19}$$

Enforcing this boundary condition it is easily shown that the functions $Y_m(\eta)$ may be expressed as

For $\lambda^2 > ((m-1)\pi)^2$:

$$Y_m(\eta) = A_m[\cosh \beta_m \eta + \theta_{1m} \cos \gamma_m \eta]. \tag{20}$$

For $\lambda^2 < ((m-1)\pi)^2$:

$$Y_m(\eta) = A_m[\cosh \beta_m \eta + \theta_{2m} \cosh \gamma_m \eta], \tag{21}$$

where

$$\theta_{1m} = \frac{[-\beta_m(\beta_m^2 - v^*\phi^2((m-1)\pi)^2)\sinh \beta_m]}{[\gamma_m(\gamma_m^2 + v^*\phi^2((m-1)\pi)^2)\sin \gamma_m]}$$

and

$$\theta_{2m} = \frac{[-\beta_m(\beta_m^2 - v^*\phi^2((m-1)\pi)^2)\sinh \beta_m]}{[\gamma_m(\gamma_m^2 - v^*\phi^2((m-1)\pi)^2)\sinh \gamma_m]}.$$

Finally, the condition of imposed harmonic edge-rotation along the driven edge is enforced. Let the amplitude of the distributed harmonic edge rotation be expressed as

$$\left.\frac{\partial W}{\partial \eta}\right|_{\eta=1} = \sum_{m=1}^{\infty} E_m \cos(m-1)\pi\xi. \tag{22}$$

Utilizing Eqs. (20) and (21), and enforcing the above boundary condition, gives

For $\lambda^2 > ((m-1)\pi)^2$:

$$Y_m(\eta) = E_m\theta_{11m}\{\cosh \beta_m \eta + \theta_{1m} \cos \gamma_m \eta\}. \tag{23}$$

For $\lambda^2 < ((m-1)\pi)^2$:

$$Y_m(\eta) = E_m\theta_{22m}\{\cosh \beta_m \eta + \theta_{2m} \cosh \gamma_m \eta\}, \tag{24}$$

where

$$\theta_{11m} = \frac{1.0}{[\beta_m \sinh \beta_m - \theta_{1m}\gamma_m \sin \gamma_m]}$$

and

$$\theta_{22m} = \frac{1.0}{[\beta_m \sinh \beta_m + \theta_{2m}\gamma_m \sinh \gamma_m]}$$

Thus, the exacot solution for response of the first building block subjected to any number of driving terms is available.

The second building block of Fig. 2 differs from the first only in that it is driven along the edge, $\xi = 1$. It is well known that the solution for this second building block can be extracted from that of the first by simply replacing the parameter λ^2 with $\lambda^2\varphi^2$, interchanging the variables ξ and η, and then replacing the aspect ratio φ with its inverse.

Solution for the second building block is expressed in series form as

$$W(\xi,\eta)=\sum_{n=1}^{\infty}Y_n(\xi)\cos(n-1)\pi\eta, \tag{25}$$

where the subscript 'n' is introduced to avoid confusion with the previous building block solution.

The functions $Y_n(\xi)$ are expressed as

For $\lambda^2\ \varphi^2>((n-1)\pi)^2$:

$$Y_n(\xi)=E_n\theta_{11n}\{\cosh\beta_n\xi+\theta_{1n}\cos\gamma_n\xi\}. \tag{26}$$

For $\lambda^2\varphi^2<((n-1)\pi)^2$:

$$Y_n(\xi)=E_n\theta_{22n}\{\cosh\beta_n\xi+\theta_{2n}\cosh\gamma_n\xi\}. \tag{27}$$

As indicated, the quantities θ_{1n}, θ_{11n}, etc., are extracted from corresponding quantities related to the first building block solution.

The third building block of Fig. 2 differs from the first, only in that the driven edge is free of bending moment and is driven by a distributed harmonic vertical edge reaction. Amplitude of this vertical edge reaction is expressed as

$$\frac{Vb^3}{aD}=\sum_{m=1,2}^{\infty}E_{m1}\cos(m-1)\pi\xi. \tag{28}$$

Solution for response of this building block is obtained in a manner exactly analogous to that described for the first building block. The dimensionless bending moment along the edge, $\eta=1$, is expressed as [5]

$$\frac{Mb^2}{aD}=-\left\{\frac{\partial^2W(\xi,\eta)}{\partial\eta^2}+\nu\phi^2\frac{\partial^2W(\xi,\eta)}{\partial\xi^2}\right\}. \tag{29}$$

Solution for this third building block takes a form identical to that given by Eqs. (15), (20) and (24), with coefficients E_m replaced by E_{m1}. The only difference relates to the quantities θ_{1m}, θ_{11m}, etc., whose counterparts are now designated by a prime symbol and become

$$\theta'_{1m}=\frac{(\beta_m^2-\nu\phi^2((m-1)\pi)^2)\cosh\beta_m}{(\gamma_m^2+\nu\phi^2((m-1)\pi)^2)\cos\gamma_m}$$

and

$$\theta'_{2m}=-\frac{(\beta_m^2-\nu\phi^2((m-1)\pi)^2)\cosh\beta_m}{(\gamma_m^2-\nu\phi^2((m-1)\pi)^2)\cosh\gamma_m},$$

$$\theta'_{11m}=-\frac{1.0}{[\beta_m(\beta_m^2-\nu^*\phi^2((m-1)\pi)^2\sinh\beta_m+\theta'_{1m}\gamma_m(\gamma_m^2+\nu^*\phi^2((m-1)\pi)^2)\sin\gamma_m]}$$

and

$$\theta'_{22m}=-\frac{1.0}{[\beta_m(\beta_m^2-\nu^*\phi^2((m-1)\pi)^2)\sinh\beta_m+\theta'_{2m}\gamma_m(\gamma_m^2-\nu^*\phi^2((m-1)\pi)^2)\sinh\gamma_m]}.$$

The fourth building block differs from the third, only in that it is moment free and driven along the edge, $\xi = 1$. Its solution is extracted from the third in a manner identical to that described for extracting the second building block solution from that of the first.

The fifth building block has a condition of zero edge rotation imposed along the edge, $\eta = 1$. This condition is denoted in the building block figures by two solid dots joined by a short straight line. It is driven by a concentrated harmonic force located dimensionless distance ζ from the η-axis. The concentrated force is essentially a concentrated vertical edge reaction. The vertical edge reaction is represented by a Dirac function expanded in an appropriate trigonometric series. This approach to obtaining the response of building blocks subjected to a concentrated force has been discussed extensively in Refs. [5,6].

Again, for this building block, the solution takes the form provided by Eqs. (15), (16) and (17). Of the two non-zero constants to be evaluated, the first is obtained by enforcement of the zero edge rotation condition discussed immediately above. Using the symbols C'_{1m} and C'_{2m}, solutions for the functions $Y_m(\eta)$ become

For $\lambda^2 > ((m-1)\pi)^2$:

$$Y_m(\eta) = A_m\{\cosh\beta_m\eta + C'_{1m}\cos\gamma_m\eta\}. \tag{30}$$

For $\lambda^2 < ((m-1)\pi)^2$:

$$Y_m(\eta) = A_m\{\cosh\beta_m\eta + C'_{2m}\cosh\gamma_m\eta\}, \tag{31}$$

where

$$C'_{1m} = \beta_m\sinh\beta_m/\gamma_m\sin\gamma_m \quad \text{and} \quad C'_{2m} = -\beta_m\sinh\beta_m/\gamma_m\sinh\gamma_m.$$

In the next step the driving vertical edge reaction is expanded in a cosine series as [5]

$$V(\xi) = P\sum_{m=1,2}^{\infty}\frac{2.0}{a\delta_m}\cos(m-1)\pi\zeta\cos(m-1)\pi\xi \tag{32}$$

where $\delta_m = 2$, for $m = 1$, and $\delta_m = 1$, for $m > 1$.

The above quantity is expressed in dimensionless form as

$$\frac{V(\xi)b^3}{aD} = P^*\sum_{m=1,2}^{\infty}\frac{2\cos(m-1)\pi\zeta}{\delta_m}\cos(m-1)\pi\xi, \tag{33}$$

where $P^* = Pb^3/a^2D$

Combining Eqs. (19) and (33) it is readily shown that the functions $Y_m(\eta)$ may be written as

For $\lambda^2 > ((m-1)\pi)^2$:

$$Y_m(\eta) = C_{1m}\{\cosh\beta_m\eta + C'_{1m}\cos\gamma_m\eta\}. \tag{34}$$

For $\lambda^2 < ((m-1)\pi)^2$:

$$Y_m(\eta) = C_{2m}\{\cosh\beta_m\eta + C'_{2m}\cosh\gamma_m\eta\}, \tag{35}$$

where

$$C_{1m} = \frac{-2\cos(m-1)\pi}{[(\beta_m(\beta_m^2 - v^*\phi^2((m-1)\pi)^2)\sinh\beta_m + C'_{1m}\gamma_m(\gamma_m^2 + v^*\phi^2((m-1)\pi)^2)\sin\gamma_m)/\delta_m]}$$

and

$$C_{2m} = \frac{-2\cos(m-1)\pi}{[(\beta_m(\beta_m^2 - v^*\phi^2((m-1)\pi)^2)\sinh\beta_m + C'_{2m}\gamma_m(\gamma_m^2 - v^*\phi^2((m-1)\pi)^2)\sinh\gamma_m)/\delta_m]}.$$

Here, the value of ζ has been set equal to 1.0, as this is the only value of this parameter that will be of interest in the present analysis (corner-supported plates).

The sixth building block of Fig. 2 differs from the fifth only in that it is driven along the edge, $\xi = 1$. Its solution is easily extracted from that of the fifth building block through interchange of the variables ξ, and η, as described earlier. One other consideration is necessary. The new coefficients $C'_{1\eta}$ and C'_{2n} must be divided by the quantity φ^4. This is necessary in view of the definition of P^*, the dimensionless concentrated driving force [5].

Before describing generation of the eigenvalue matrix it is appropriate to look briefly at building block solutions required for analysis of the fully antisymmetric, and symmetric–antisymmetric modes.

2.3. Analysis of fully antisymmetric modes

This family of modes is analyzed by means of the building blocks of Fig. 3. They differ from those of Fig. 2 only in that the edges, $\xi = 0$, and $\eta = 0$, are given simple instead of slip-shear support.

It will be obvious, referring to Eq. (15), that solution for the first building block of this set can be written as

$$W(\xi,\eta) = \sum_{m=1,2}^{\infty} Y_m(\eta)\sin(2m-1)\pi\xi/2. \tag{36}$$

Note that for all building blocks of this set the sine series above replaces the cosine series of the earlier set. It will also be appreciated that the symmetric rather than the antisymmetric terms of

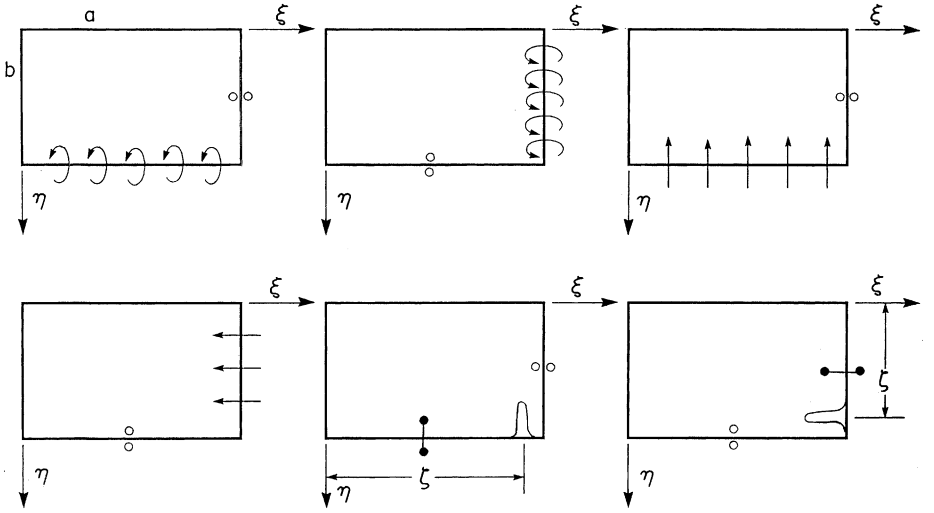

Fig. 3. Schematic representation of building blocks employed in fully antisymmetric mode analysis.

Eqs. (17) and (18), must now be deleted. Beyond these minor changes, solutions for the building blocks of Fig. 3 are now obtained in a manner identical to that described for those of Fig. 2. The reader will have no trouble obtaining these solutions.

2.4. Analysis of symmetric–antisymmetric modes

Here, the free vibration modes which are symmetric about the ξ-axis and antisymmetric about the η-axis are investigated. By properly orienting the central axis of the plate of interest, all possible modes of this family may be analyzed. The required building blocks are shown in Fig. 4. It will be noted that simple support conditions are imposed along the η-axis of each building block while slip-shear conditions are imposed along the ξ-axis. The reader will recognize that solutions for all of these building blocks are readily obtained by expressing the displacement amplitude in terms of the appropriate trigonometric series as already discussed. It is also necessary to enforce the appropriate boundary conditions in each case.

It will be noted that the solution for the sixth building block of this set cannot be extracted from the fifth, as was done for the earlier sets. This is because of the nature of the boundary conditions. In order to arrive at a solution for the sixth building block it is found advantageous to begin by obtaining the solution for the building block of Fig. 5. This is easily achieved by following the steps discussed earlier. Finally, transforming this solution by following steps discussed in connection with the fully symmetric mode analysis, one arrives at the required solution.

2.5. Development of the eigenvalue matrix

It will be seen shortly that enforcement of the appropriate quarter plate boundary conditions permits the writing of homogeneous algebraic equations relating the driving coefficients appearing

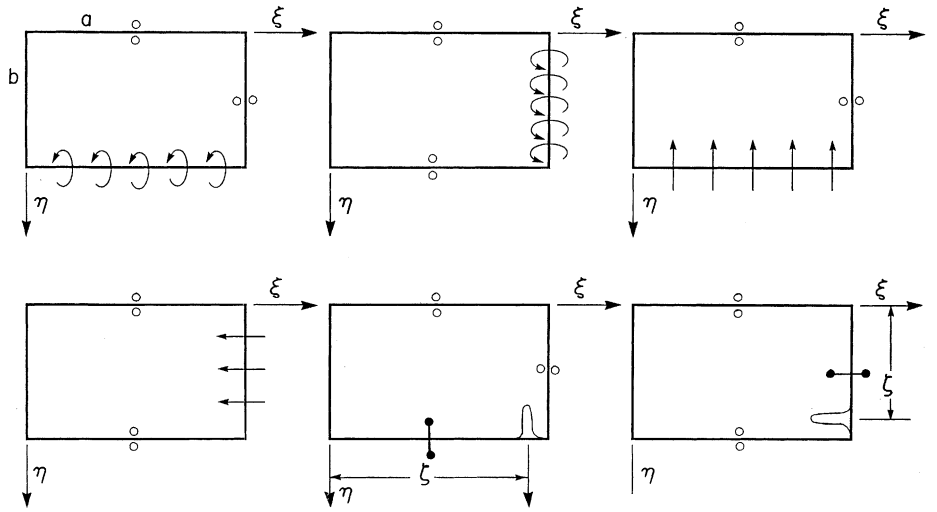

Fig. 4. Schematic representation of building blocks employed in symmetric–antisymmetric mode analysis.

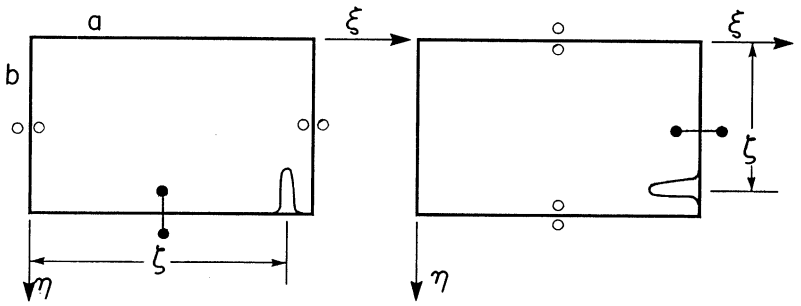

Fig. 5. Schematic representation of intermediate building block employed in order to arrive at solution for building block of ultimate interest.

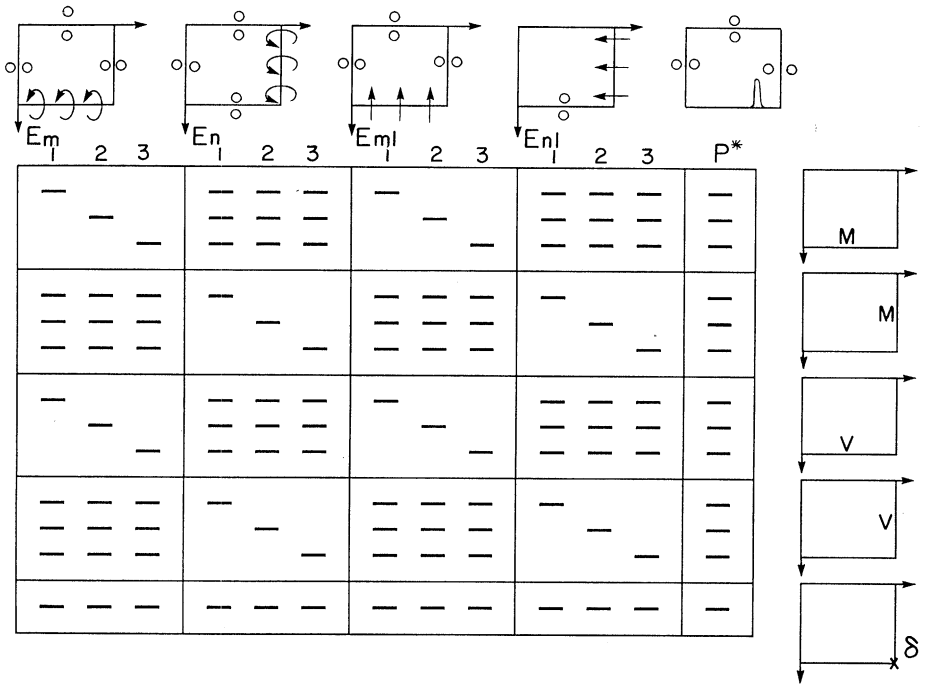

Fig. 6. Schematic representation of eigenvalue matrix based on three-term solutions for building blocks

in the building block solutions for each of the three mode families. The eigenvalue matrix for each family is, in fact, the coefficient matrix for the related set of these homogeneous equations. The form of the associated eigenvalue matrix will be identical for each family. We begin by describing generation of the matrix for fully symmetric mode analysis.

The actual matrix, based on three-term solutions for building blocks, is depicted schematically in Fig. 6. Small figures across the top indicate building blocks employed. Inserts along the right-hand side indicate boundary conditions to be satisfied and the edge to which they apply. Letters M and V indicate moment and vertical edge reaction equilibrium, respectively. The symbol δ at the

lower right-hand corner indicates that displacement of the quarter plate of interest must equal zero at this corner of the plate.

Initially the driving coefficients, E_m, E_n, etc., are constrained so that the condition of moment equilibrium is satisfied along the edge, $\eta = 1$. Reviewing the boundary conditions related to this edge it is seen that the net displacement of the superimposed building blocks must satisfy the condition

$$\frac{Mb^2}{aD} + G_{11}\frac{\partial^2}{\partial\xi^2}\frac{\partial W(\xi,\eta)}{\partial\eta} + G_{12}\frac{\partial W(\xi,\eta)}{\partial\eta} = 0, \tag{37}$$

where

$$\frac{Mb^2}{aD} = -\left\{\frac{\partial^2 W(\xi,\eta)}{\partial\eta^2} + v\phi^2\frac{\partial^2 W(\xi,\eta)}{\partial\xi^2}\right\}.$$

Standard procedures are followed in enforcing the boundary condition as expressed by Eq. (37). The contribution of each building block to the left-hand side of this equation is expanded in an appropriate Fourier series. Here the cosine series is appropriate. The net coefficient of each term in this new series (including all the building block contributions) is set equal to zero. This gives rise to a set of K homogeneous algebraic equations relating the $(4K+1)$ building block driving coefficients, where K equals the number of terms utilized in the building block solutions.

Short bars in the first three rows of the matrix of Fig. 6 represent coefficients of this set of homogeneous equations. It will be noted that some segments of this matrix contain diagonal terms only. This is because contributions from building blocks related to these segments, including contributions of the first building block, are already available in a cosine series and off-diagonal matrix elements equal zero.

The second row of matrix segments relate to the condition of moment equilibrium along the edge, $\xi = 1$.

This equilibrium condition is expressed as

$$\frac{Ma}{D} + G_{21}\frac{\partial^2}{\partial\eta^2}\frac{\partial W(\xi,\eta)}{\partial\xi} + G_{22}\frac{\partial w(\xi,\eta)}{\partial\xi} = 0, \tag{38}$$

where

$$\frac{Ma}{D} = -\left\{\frac{\partial^2 W(\xi,\eta)}{\partial\xi^2} + \frac{v}{\phi^2}\frac{\partial^2 W(\xi,\eta)}{\partial\eta^2}\right\}.$$

Generation of the matrix elements associated with this boundary condition proceeds in a manner almost identical to that described above for the edge, $\eta = 1$. Again a cosine series is utilized for the Fourier expansion. The single difference relates to generation of elements of the right-hand column of the matrix. It is found advantageous to now utilize the solution of the sixth building block in the set as discussed earlier. In this way contributions of the concentrated-force-driven building block are already available in a cosine series. The need to perform a Fourier expansion of the bending moment contribution is therefore eliminated.

The third set of equations utilized to construct the eigenvalue matrix are based on satisfaction of vertical edge reaction equilibrium along the edge, $\eta = 1$. The equation to be satisfied takes

the form

$$\frac{Vb^3}{aD} + Q_{11}\frac{\partial^4 W(\xi,\eta)}{\partial\xi^4} - Q_{12}W(\xi,\eta) = 0, \tag{39}$$

where

$$\frac{Vb^3}{aD} = -\left\{\frac{\partial^3 W(\xi,\eta)}{\partial\eta^3} + v^*\phi^2\frac{\partial^3 W(\xi,\eta)}{\partial\eta\partial\xi^2}\right\}.$$

Again, a cosine series is utilized for expansion of the left-hand side of this equation. The first term of the equation is taken care of by simply adding the quantity unity to each of the elements lying on the main diagonal of the matrix.

Focusing on the second term of Eq. (39) it is seen that a Fourier expansion procedure must be utilized in obtaining the contributions of the second and fourth building blocks. Following conventional procedures one would take the fourth derivative of displacement with respect to the variable ξ and then expand it in a cosine series. Experience has shown that better convergence is obtained by following an alternate procedure. First the displacement is expanded in a Fourier series and then take the fourth derivative of each term in the series is taken. This is the procedure that has been followed here.

The fourth set of equations utilized to construct the eigenvalue matrix are based on satisfaction of vertical edge reaction equilibrium along the edge, $\xi = 1$. The equation to be satisfied takes the form

$$\frac{Va^2}{D} + Q_{21}\frac{\partial^4 W(\xi,\eta)}{\partial\eta^4} - Q_{22}W(\xi,\eta) = 0, \tag{40}$$

where

$$\frac{Va^2}{D} = -\left\{\frac{\partial^3 W(\xi,\eta)}{\partial\xi^3} + \frac{v^*}{\phi^2}\frac{\partial^3 W(\xi,\eta)}{\partial\xi\partial\eta^2}\right\}.$$

Matrix elements based on this equation are generated in a manner completely analogous to those generated in connection with Eq. (39).

Finally, the last row of elements in the eigenvalue matrix are based on the requirement that the sum of all building block contributions toward lateral displacement at the quarter plate outer corner must equal zero. The appropriate matrix elements are easily generated.

Eigenvalue matrices related to fully antisymmetric and symmetric–antisymmetric free vibration modes are generated in a manner identical to that described above for fully symmetric modes. Of course, the appropriate building block solutions must be utilized for the family of modes under study.

With the eigenvalue matrices available for any mode family, eigenvalues are computed following well-established procedures. Eigenvalues are those values of the parameter λ^2, which cause the determinant of the eigenvalue matrix to vanish. After conducting an eigenvalue search the mode shape associated with any eigenvalue is obtained by setting one of the non-zero driving

coefficients equal to unity and solving the resulting set of non-homogenous algebraic equations for the remaining driving coefficients. Mode shapes are then generated.

3. Computed free vibration results

The first step necessary, before beginning computation of free vibration eigenvalues, is to decide on the number of terms to be utilized in the building block solutions. This, in turn, depends upon the number of significant digits required in the computed results. It is known that in the analysis of plate vibration problems where Dirac functions are utilized, the rate of convergence will be slower. Consequently, one must begin with convergence tests.

Typical convergence curves are shown in Figs. 7 and 8. They represent studies of first fully antisymmetric mode free vibration of a square corner-supported plate. The results of Fig. 7 were obtained with all edge-beam coefficients set equal to zero. The first mode eigenvalue for this problem was obtained in an earlier and simpler study involving plates with corner supports only [7]. At that time the eigenvalue was reported as 9.546. In fact, the value obtained here, using the extra building blocks required for edge-beam vibration tests, is identical. This serves as an excellent check on the present computational procedure. It will also be noted that, based on the plotted results, a value of 35 for the parameter K would guarantee three digit accuracy and in most cases provide up to four digit accuracy.

A similar convergence curve is plotted in Fig. 8. Here the input parameters related to lateral and rotary inertia are set equal to zero while dimensionless lateral and rotational stiffness parameters, Q_{11}, Q_{21}, G_{11}, and G_{21}, are arbitrarily set equal to 200. It is seen that the convergence

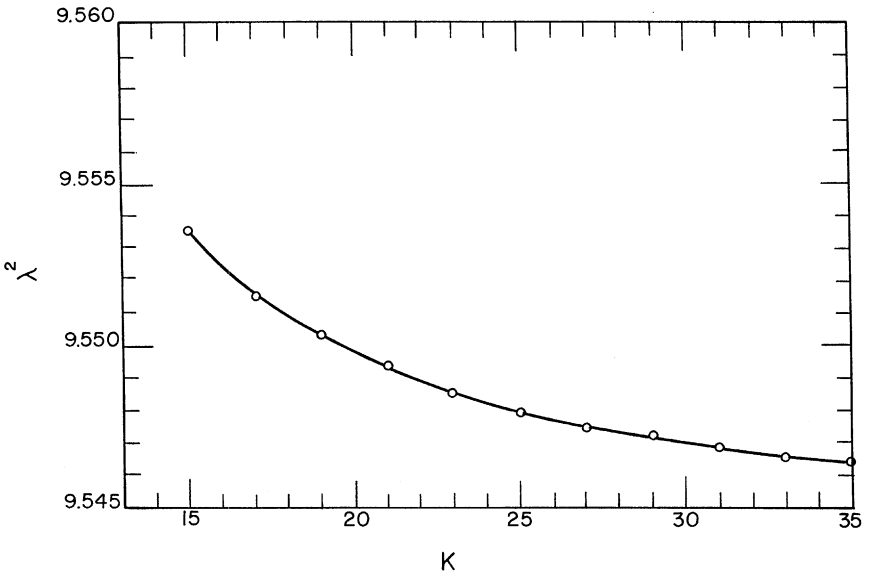

Fig. 7. Plot of convergence curve associated with first fully antisymmetric mode analysis of corner-supported plate without edge-beam reinforcement.

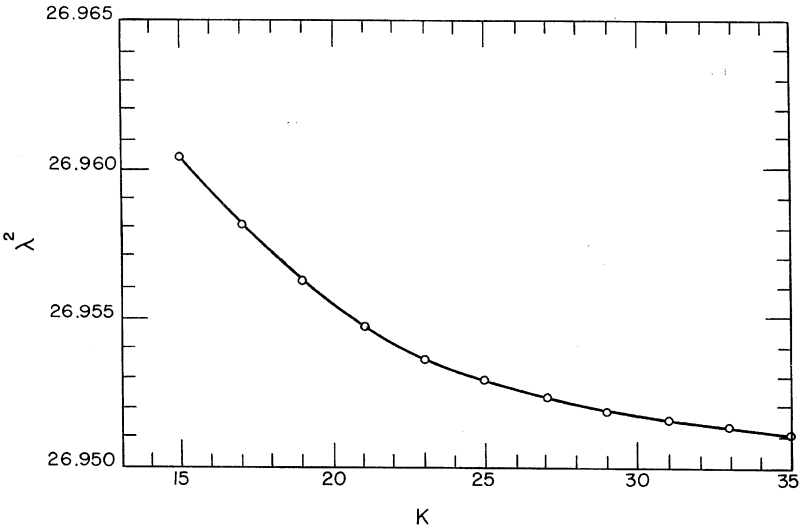

Fig. 8. Plot of convergence curve associated with first fully antisymmetric mode analysis of corner-supported plate with edge-beam reinforcement. All beam stiffness coefficients equal 200. Effects of beam lateral and rotary inertia neglected.

rate represented by Fig. 8 is as good as, or better, than that of Fig. 7. In view of the above findings it was decided to utilize 35 terms in all building block solutions when computing results plotted here. Results presented in digital form were computed while utilizing 90 terms in the building block solutions.

As indicated earlier, there are many verification tests which can be performed to test the validity of the present analysis. Results of two such validation tests involving first doubly antisymmetric mode vibration of a square plate are presented in Figs. 9 and 10. Identical edge beams are considered to be attached along all plate edges.

In Fig. 9 the free vibration eigenvalue is plotted against the edge-beam lateral stiffness parameter Q_{11}. Effects of beam rotational stiffness and lateral and rotational inertia are neglected. It will be obvious that in this case the lower eigenvalue limit must equal 9.546 as discussed above. The upper limit to be approached must equal that related to a square plate with simple support along all edges, i.e., a value of $2\pi^2$. It is seen in Fig. 9 that in fact the plotted curve begins at the correct value and approaches arbitrarily close to the known upper limit as the beam lateral stiffness is permitted to increase.

The verification test of Fig. 10 differs from that of Fig. 9 only in that here the dimensionless rotational stiffness parameter G_{11} is set equal to Q_{11} instead of zero. It will be appreciated that the lower limit for the plotted eigenvalue curve will be unchanged. The upper limit, however, will now take on a value corresponding to that of first fully antisymmetric mode vibration of the fully clamped square plate. This value is known to be 27.03 [5].

A study of Fig. 10 reveals that, in fact, the plotted curve begins at the correct lower limit value and approaches arbitrarily close to the known upper limit as the stiffness parameters are allowed to increase. These tests constitute valuable checks on the mathematical procedure employed.

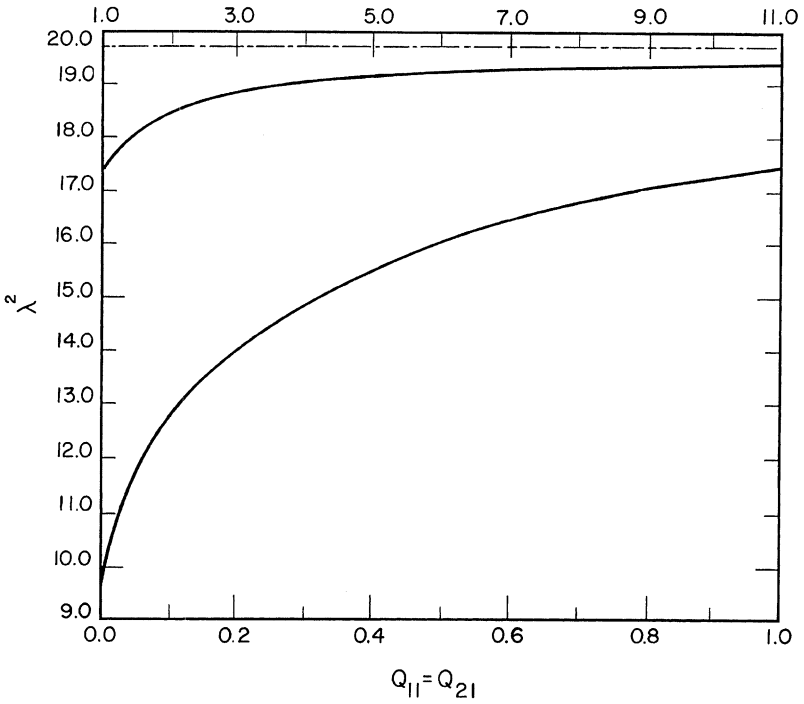

Fig. 9. Plot of eigenvalue vs. parameter Q_{11} for first double antisymmetric mode vibration of edge-beam reinforced square plate, $Q_{11} = Q_{21}$. All other beam–plate interaction parameters equal zero.

A number of similar tests have been conducted where only the dimensionless coefficients related to lateral and rotational inertia have been allowed to vary. It is demonstrated in fundamental mode analysis, for example, that increase of either of these parameters causes the eigenvalue to decrease toward zero.

In order to further demonstrate exploitation of the analytical method described, and to provide other researchers and designers with digital results against which their findings may be compared, it was decided to perform a free vibration analysis of a plate with edge beams, of two different but realistic geometries.

Consider the schematic representation of an edge beam as depicted in Fig. 11. The beam is of rectangular cross-section with a depth-to-width ratio of 3.0. We will denote the width as αh, where h equals the plate thickness. Both plate and beam are considered to be fabricated from the same isotropic material. In order to define the problem consider a square plate with an edge length-to-thickness ratio of 96. This corresponds, for example, to a plate, 12 in on the edge with a thickness of 1/8 in, although results apply to any square plate with this length-to-thickness ratio.

It is considered that identical beams are attached to each plate edge during any computational analysis. The first three eigenvalues will be computed for each of the three mode families, as discussed earlier. Attention will be focused on two different values for the edge-beam width parameter, α.

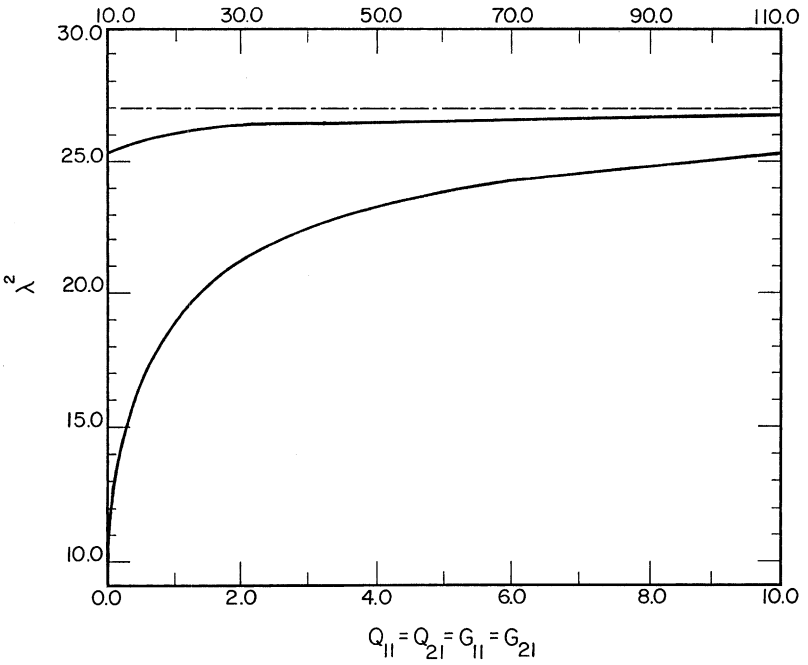

Fig. 10. Plot of eigenvalue vs. parameter Q_{11} for first doubly antisymmetric mode vibration of edge-beam reinforced square plate, $Q_{11} = Q_{21} = G_{11} = G_{21}$. Beam inertia effects neglected.

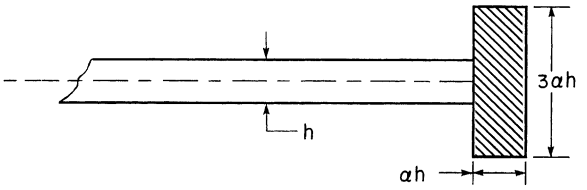

Fig. 11. View of section taken through plate and beam for illustrative problem.

Before beginning the computations it is necessary to assign values to the beam stiffness and inertia properties. It will be recalled that the shear modulus, G, is expressed as $E/2(1+v)$.

Furthermore, temporarily denoting the beam width and depth as, b and d, respectively, it is shown that the polar moment of inertia of the beam cross-section becomes

$$J = (bd^3 + db^3)/12. \tag{41}$$

The moment of inertia of the beam cross-section in torsion may be obtained from the work of Timoshenko and Goodier [8]. They have shown that, for a beam of rectangular cross-section, with the above dimensions, the moment in torsion may be written as

$$M_t = G\theta\, k_1 b^3 d, \tag{42}$$

where, for a ratio d/b equal to 3.0, the value of k_1 equals 0.263. The equivalent moment of inertia in torsion, J_0, then becomes $k_1 b^3 d$.

Utilizing these quantities, and returning temporarily to the definitions, Q_{11}, G_{11}, etc., as developed earlier, it is shown that for the edge-beam reinforced plates of current interest we may write

$$Q_{11} = 27\alpha^4(1-v^2)/96, \quad G_{11} = 4.734\alpha^4(1-v)/96,$$
$$Q_{12} = 3\alpha^2\lambda^4/96, \quad G_{12} = 2.5\alpha^4\lambda^4/(96)^3, \tag{43}$$

where the role of the plate length-to-thickness ratio, 96, has been separated out.

Eigenvalues are computed for two values of the beam geometric parameter, α, i.e., 1.0, and 1.5. Results are tabulated in Tables 1–3.

Setting the value of α equal to zero corresponds to the situation where the corner-supported plate has no edge-beam reinforcement. This has been done for each mode studied and in each case excellent agreement between computed eigenvalues and those of Ref. [6] has been obtained.

Two eigenvalues have been tabulated for each of the three modes listed in Tables 1–3. The first eigenvalue, λ^{2*}, corresponds to the situation where the beams provide elastic lateral and rotational support only, i.e., inertia effects are neglected. In computing the second eigenvalue, λ^2, both elastic and inertia effects are included. In this way it is possible to immediately determine how much error would be introduced through neglecting inertia effects. It will also be appreciated that eigenvalues obtained with α equal zero act as lower limits for the eigenvalues λ^2.

It will be observed in the tables provided that edge-beam inertia effects are extremely small in first mode vibration of each family. Moving up to the higher modes, however, it is noted that the inertia effects quickly become significant. This is to be expected as, in the higher modes, the beam cross-section dimensions become more and more significant in comparison with inter node line distances of the vibrating plate.

Pairs of selected quarter-plate mode shapes are presented, for square plates, in Figs. 12–14. Each figure pertains to the first mode of vibration, one figure for each of the three mode families studied. The laterally supported plate corner is located in the immediate foreground in each figure. Lateral displacement is, of course, zero at this location. In generating the (a) portion of the figures the parameter α has been set equal to zero, while, for the (b) portion, it has been set

Table 1
Computed fully symmetric mode eigenvalues for corner supported plate with edge-beams

Mode	α	λ^{2a}	λ^2
1	1.0	3.364	3.342
	1.5	4.535	4.516
2	1.0	9.066	8.493
	1.5	16.74	15.23
3	1.0	31.32	29.77
	1.5	37.07	32.66

[a] Implies inertia effects neglected, $a/h = 96$.

Table 2
Computed fully antisymmetric mode eigenvalues for corner supported plate with edge-beams

Mode	α	λ^{2a}	λ^2
1	1.0	15.05	14.82
	1.5	19.08	18.91
2	1.0	27.73	25.68
	1.5	40.74	37.73
3	1.0	37.27	35.46
	1.5	45.05	42.59

[a] Implies inertia effects neglected, $a/h = 96$.

Table 3
Symmetric–antisymmetric mode eigenvalues for corner supported plate with edge-beams

Mode	α	λ^{2a}	λ^2
1	1.0	6.905	6.696
	1.5	9.952	9.653
2	1.0	18.28	17.21
	1.5	23.86	20.84
3	1.0	24.80	23.88
	1.5	30.57	29.74

[a] Implies inertia effects neglected, $a/h = 96$.

equal to 1.5. All beam inertia effects are included. The objective in presenting these mode shapes has been to enable the reader to observe the actual influence of the edge beams on these shapes.

In each case the stiffening effects of the edge beams is evident, particularly as it relates to the plate lateral displacement along the stiffened edges. This stiffening effect is particularly apparent in Fig. 13. With sufficient increase in the parameter α the outer edges in the latter figure will approach a clamped edge condition. These stiffening effects are also particularly apparent along the outer edge to the viewer's left in Fig. 14.

4. Discussion and conclusions

It is well demonstrated in the literature that the superposition method has the capacity to obtain accurate analytical type solutions for the free vibration of rectangular plates with elastic lateral and rotational support running along the outer boundaries [9,10]. In this paper it is demonstrated that the same method has the capacity to handle the more complicated problems related to plates

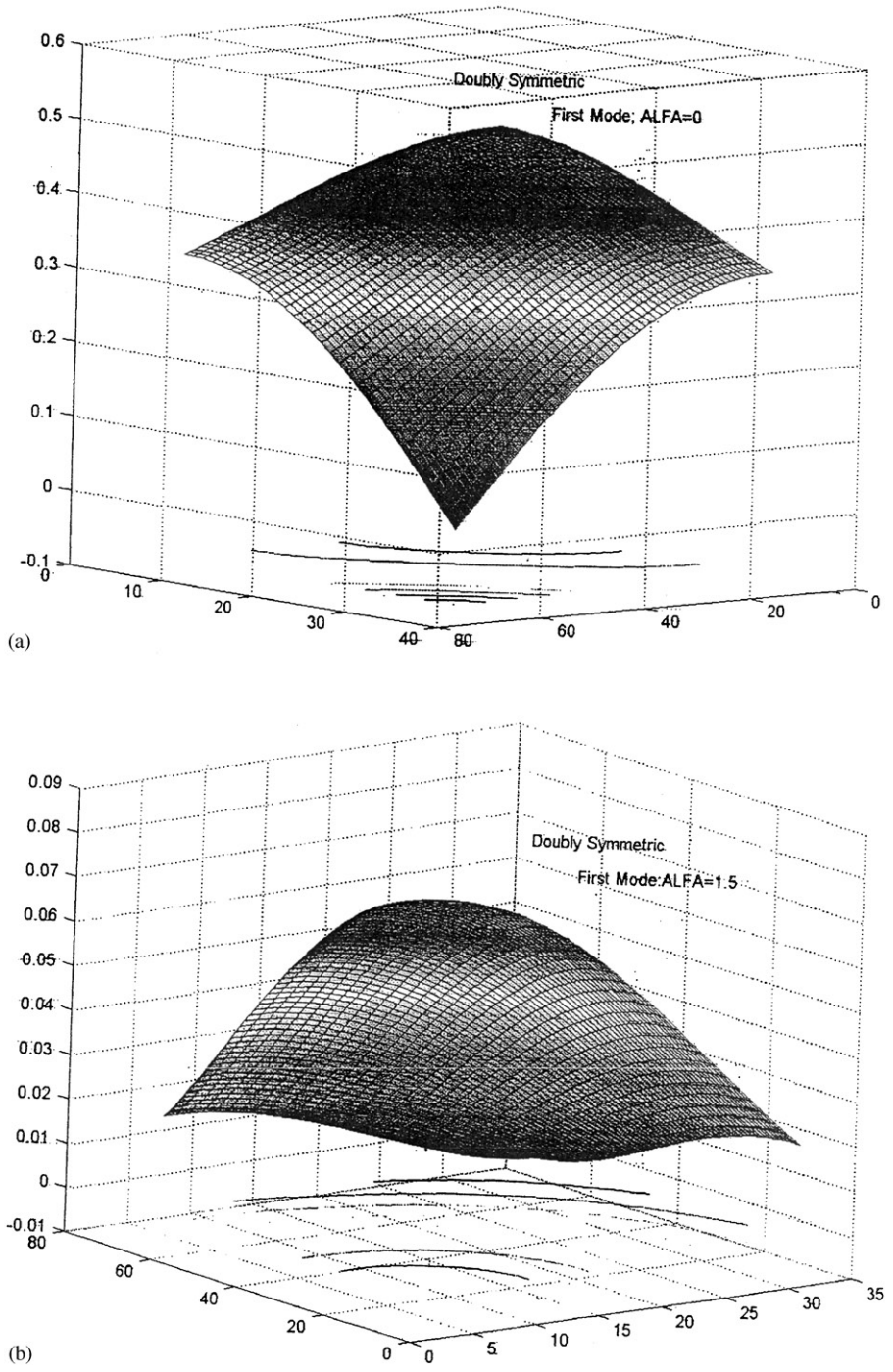

Fig. 12. Computed mode shape for square quarter plate in first doubly symmetric mode vibration. (a) Without edge-beam reinforcement. (b) With edge-beam reinforcement ($\alpha = 1.5$).

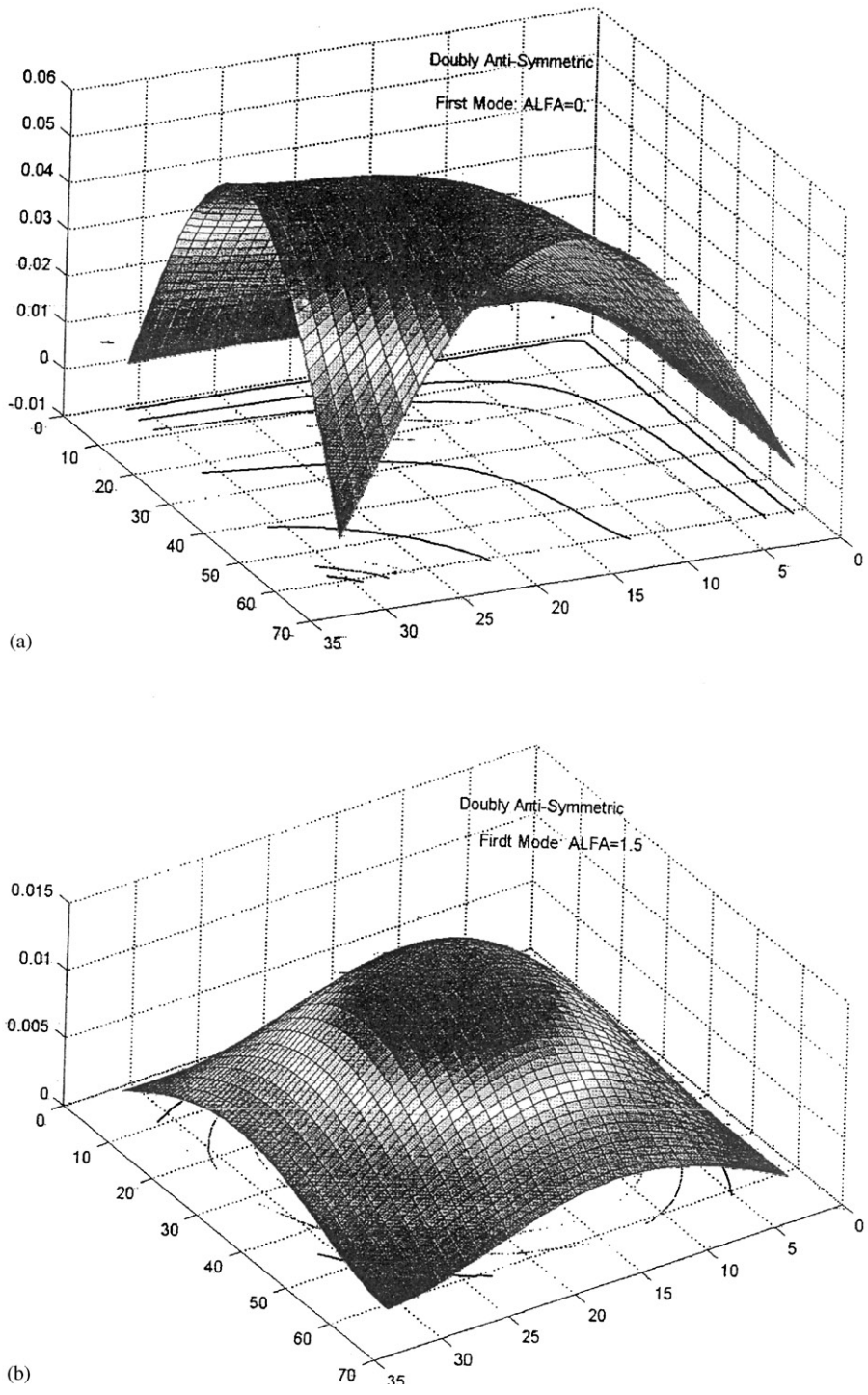

Fig. 13. Computed mode shape for square quarter plate in first doubly antisymmetric mode vibration. (a) Without edge-beam reinforcement. (b) With edge-beam reinforcement ($\alpha = 1.5$).

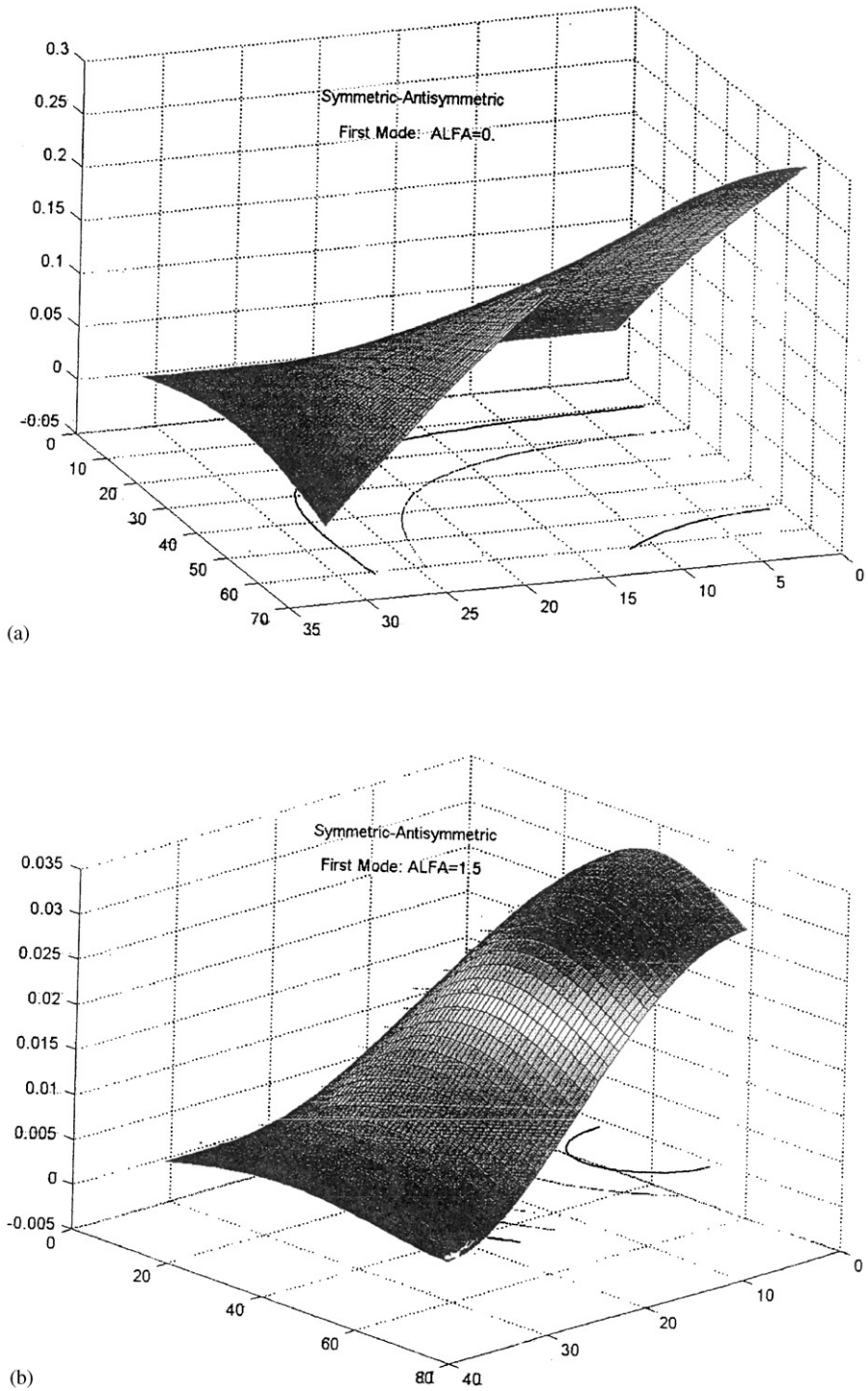

Fig. 14. Computed mode shape for square quarter plate in first symmetric–antisymmetric mode vibration. (a) Without edge-beam reinforcement. (b) With edge-beam reinforcement ($\alpha = 1.5$).

with elastic beams attached to the same boundaries. All plate–beam interaction parameters arising in connection with beam stiffness and inertia have been developed and presented in dimensionless form. Verification tests associated with known frequency limits that must be approached as beam stiffnesses are increased arbitrarily, have been conducted. It is demonstrated that effects of beam lateral and rotational inertia are easily included, or deleted, in the analysis. This permits the analyst to decide whether or not such effects may be neglected for the purposes of a particular design.

It was demonstrated that edge beams of certain realistic geometries can have significant effects on raising natural frequencies of corner-supported plates. This may be of interest in the design of electronic circuit boards, for example, where it is often desired to increase the fundamental frequency beyond certain pre-set levels.

Finally, the question may arise as to how one would handle similar problems where the edge-beam properties do not possess symmetry with respect to their distribution about the plate central axes. An example of such a plate would be one where beams of different properties run along each of the four edges. The reader may wish to examine the set of building blocks utilized in analyzing the fully symmetric modes of the present plate (Fig. 2). It will be appreciated that replacing the quarter-plate with the full plate and coupling the above set of building blocks with an additional set driven along the other two plate edges will permit the desired general analysis to be achieved. Building block solutions for the additional set will be extracted from those of the first set.

In summary, it appears that the present work constitutes the first comprehensive analytical type solution to the problem of free vibration of corner-supported rectangular plates with symmetrically distributed edge-beam reinforcement.

Appendix A. Nomenclature

a, b	edge dimensions of quarter-plate
A_B	cross-sectional area of edge beam
D	plate flexural rigidity $= Eh^3/12(1-v^2)$
E	Young's modulus of plate material
E_B	Young's modulus of beam material
G	beam modulus of elasticity in shear
h	plate thickness
I	area moment of inertia of beam cross-section
J	polar moment of inertia of beam cross-section
J_0	moment of inertia of beam cross-section in torsion
K	number of terms utilized in building block solutions
M	plate bending moment
M_t	torsional moment in beam
m	mass of beam per unit length
P	amplitude of concentrated harmonic driving force
P^*	$= Pb^3/a^2D$
$Q_{11}, Q_{21}\ldots$, $G_{11}, G_{21}\ldots$, etc.,	beam–plate interaction coefficients defined in text

t	time
V	plate vertical edge reaction
w	plate lateral displacement
W	$= w/a$
x, y	co-ordinates measured along edges of quarter-plate
v	the Poisson ratio (taken as 0.333 in computations reported here)
v^*	$= (2 - v)$
$\xi, \eta,$	$= x/a$, and y/b, respectively
ω	circular frequency of vibration
ρ	mass of plate per unit area
ρ_P	density of plate material
ρ_B	density of beam material
λ^2	vibration eigenvalue $= \omega a^2\sqrt{\rho/D}$
φ	plate aspect ratio, b/a
α	illustrative edge-beam width $= \alpha h$

References

[1] H.L. Cox, W.A. Benfield, Vibration of uniform plates bounded by flexible beams, Journal of the Acoustical Society of America 31 (7) (1959) 963.

[2] I. Elishakoff, A. Sternberg, Vibration of rectangular plates with edge-beams, Acta Mechanica 36 (1980) 195–212.

[3] I. Elishakoff, Y.K. Lin, L.P. Xhu, Probabilistic and Convex Modeling of Acoustically Excited Structures, Elsevier, Amsterdam, Netherlands, 1994 (Chapter VIII).

[4] S. Timoshenko, S. Woinowsky-Krieger, Theory of Plates and Shells, McGraw-Hill, New York, 1959.

[5] D.J. Gorman, Free Vibration Analysis of Rectangular Plates, Elsevier, North-Holland, New York, 1982.

[6] D.J. Gorman, Vibration Analysis of Plates by the Superposition Method, World Scientific, NJ, USA, 1999.

[7] D.J. Gorman, A note on the free vibration of rectangular plates resting on symmetrically distributed point supports, Journal of Sound and Vibration 131 (3) (1989) 515–519.

[8] S. Timoshenko, J.N. Goodier, Theory of Elasticity, 3rd Edition, McGraw-Hill, New York, 1987.

[9] D.J. Gorman, A general solution for the free vibration of rectangular plates resting on uniform elastic edge supports, Journal of Sound and Vibration 139 (2) (1990) 325–335.

[10] D.J. Gorman, A general solution for the free vibration of rectangular plates with arbitrarily distributed lateral and rotational elastic edge support, Journal of Sound and Vibration 174 (4) (1994) 451–459.